Acid sites modulation of siliceous-based mesoporous material by post synthesis methods

Pizzolitto, Cristina; Ghedini, Elena; Taghavi, Somayeh; Menegazzo, Federica; Cruciani, Giuseppe; Peurla, Markus; Eränen, Kari; Heinmaa, Ivo; Aho, Atte; Kumar, Narendra; Murzin, Dmitry Yu; Salmi, Tapio; Signoretto, Michela

Published in:
Microporous and Mesoporous Materials

DOI:
10.1016/j.micromeso.2021.111459

Published: 01/12/2021

Document Version
Accepted author manuscript

Document License
CC BY-NC-ND

Acid sites modulation of siliceous-based mesoporous material by post synthesis methods

Cristina Pizzolitto[1,4,] Elena Ghedini[1], Somayeh Taghavi[1], Federica Menegazzo[1], Giuseppe Cruciani[2], Markus Peurla[3], Kari Eränen[4], Ivo Heinmaa[5], Atte Aho[4], Narendra Kumar[4], Dmitry Yu. Murzin[4], Tapio Salmi[4], Michela Signoretto[1]

[1]CATMAT Lab, Department of Molecular Sciences and Nanosystems, Ca' Foscari University of Venice and INSTM RUVe, via Torino 155, 30172 Venezia Mestre, Italy;
[2]Physics and Earth Sciences Department, University of Ferrara, Via Saragat, 1-44122 Ferrara, Italy
[3]Faculty of Medicine, Institute of Biomedicine, Turku University, 20520 Turku, Finland
[4]Laboratory of Industrial Chemistry and Reaction Engineering, Faculty of Science and Engineering, Åbo Akademi University, 20520 Turku, Finland,
[5]National Institute of Chemical Physics and Biophysics, Akadeemia tee 23, 12618 Tallinn, Estonia

Abstract

The present work is focused on the improvement of an effective approach to tailor the acidity of silica alumina composite. SBA-15 was selected based on high surface area, uniform porosity and large mesopores. Modification of SBA-15 was performed to improve both Lewis and Brønsted acidities and hence catalyst activity. Therefore, introduction of alumina as a co-catalyst was carried out to enhance Lewis acid sites through its incorporation into the silica network. Evaporation impregnation method was evaluated for incorporation of alumina to SBA-15 and materials with different SiO_2/Al_2O_3 ratios were prepared. Acidity and morphological features of the materials were assessed using XRD, EDX, SEM, TEM, N_2-physisorption, ^{27}Al MAS-NMR and FTIR with pyridine. Brønsted acidity was attained by the introduction of sulfonic acid groups in the final catalyst via the post-synthesis grafting method. Therefore, the balanced Lewis and Brønsted acidities and proper porosity of modified SBA-15 led to its efficient performance in the conversion of glucose as a biomass-based model component to levulinic acid.

Keywords Promoted SBA-15, Lewis acidity, Brønsted acidity, porosity, acid site modification

1. Introduction

Future biorefineries require application of heterogeneous catalysts [1]. Even if homogeneous catalysts have multiple advantages such as high selectivity and activity, they also exhibit problems with recyclability, corrosion, and environmental pollution [2]. The use of heterogeneous catalysts can overcome all previous limitations, reducing toxic wastes and corrosion, fostering catalyst reuse and the abatement of the overall process cost [3]. Several heterogeneous acid catalysts, including ion exchange resins, sulfonated zirconia-SBA-15 [4], sulfonated silica/carbon composites [5], zeolites [6,7] and aluminosilicates were used in biomass valorization. In the majority of mentioned application, acidity and porosity are the most important parameters that must be carefully adjusted to obtain a good selectivity and the yield of the desired product. Moreover, a proper balance between the Lewis and Brønsted acid sites should be maintained. SBA-15, an ordered mesoporous material, was efficient as the catalyst owing to its high surface area, a large pore volume and relatively good thermal and hydrothermal stability [8]. However, since both Lewis and Brønsted acid sites are required for several biomass conversion processes, modification of SBA-15 should be performed. Many studies have been reported in the literature regarding synthesis of various silica-metal SBA-15 type composites [9]. Kilos *et al*. have studied incorporation of different transition metals including Nb, V and Mo into SBA-15. It was demonstrated that location of the metals in SBA-15 (framework or extra-framework), the texture, morphology and acidity of the metal- modified SBA-15 are strongly depended on the metal nature and loading. XRD, UV-VIS and H_2-TPR analyses have shown that all metals were located in both framework and extra-framework of SBA-15. However, Nb(V)-oxide species with a high loading were mostly located in the extra-framework, while MoO_3 seemed to be mostly located inside the SBA-15 framework. FTIR-pyridine has shown that SBA-15 with a high Nb loading had a lower number of Lewis acid sites with a higher strength compared with the parent SBA-15 witch was related to a low dispersion of the metal species and hence their lower accessibility [10]. Szczodrowski *et al*. reported the doping effect of Al, Ti, Zr on acidity of SBA-15 [11] emphasising the main difficulties in the incorporation of heteroatoms due to the weak heteroatom-O-Si bond and

differences in hydrolysis rate of silica and heteroatom precursors. For this reason, alumina was selected as the promoter of SBA-15 due to similarities of the atom size with silicon and the ability to easily enter the silicon skeleton [12]. In one of our previous studies, the effect of zirconia incorporation on three different ordered silica materials such as MCM-41, MCM-48 and SBA-15 was studied and it was demonstrated that the characteristics of the final silica materials depend on their textural and chemical–physical properties, the correlation between the particle size of incorporated zirconia and the host material pore size and hence the position of zirconia in the ordered silica materials structure [13]. Herein, evaporation-impregnation have been studied using aluminium nitrate as the alumina precursor. Moreover, to further improve the surface acidic functionalities of the support, the most common technique is to add sulfonic groups via direct sulfonation [14]. However, the direct synthesis method in many cases leads to a loss of the mesoporous order of the pore architecture. Typically, introduction of sulfonic groups is carried out with a concentrated sulfonic acid upon heating [15]. An effective and sustainable alternative to the direct sulfonation method is the grafting technique implying anchoring the active functionalities onto the support surface via the covalent bonds [13,14,16]. In this work, post-synthesis evaporation impregnation and grafting methods have been selected for introduction of the Lewis and Brønsted acid sites to SBA-15, respectively.

Substantial efforts are required to move from a fossil fuel era to a renewable one [15,16]. Biomass is an attractive feedstock being carbon neutral [21]. In particular, chemocatalytic conversion of biomass into chemicals is an attractive approach to valorise lignocellulosic wastes and produce important chemical building blocks [22]. One of the most prominent biomass valorisation processes that requires the use of acid-based catalyst is levulinic acid (LA) production. Indeed, LA was defined in 2004 by the US Department of Energy as one of the top twelve bio-based building blocks because of its two main reactive groups, i.e. carbonyl and carboxyl ones, which allows conversion of LA to a wide range of different products [19,20]. Lignocellulosic biomass, in particular, cellulose, can be converted into LA via acid hydrolysis. Several steps, reported in Scheme 1, are involved in this

transformation: 1) hydrolysis of cellulose to glucose, 2) isomerisation of glucose to fructose, 3) dehydration of fructose to 5-hydroxymethylfurfural (5-HMF)and 4) rehydration of 5-HMF to LA and formic acid [21-23].

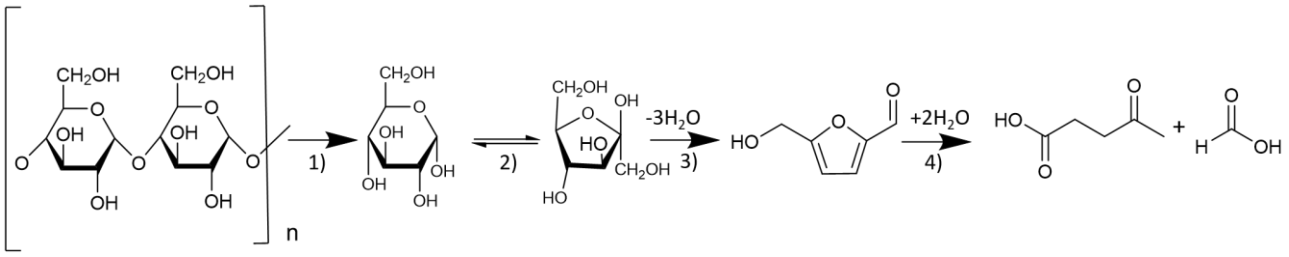

Scheme 1. Reaction pathways of cellulose conversion to levulinic acid

All these reactions are catalysed by acid sites, both Brønsted and Lewis ones [28]. In particular, the first and the last steps of the reaction are catalysed by Brønsted acid sites, the second stage is catalysed by Lewis acid sites, while the third one can be catalysed by both functionalities [29]. For this reason, the catalyst has a pivotal role in the efficiency of the entire process, since a side reaction of polycondensation can diminish LA selectivity. In particular, the acidic properties of the catalyst in terms of the amount, strength and type of acidity have vital roles in controlling the reaction pathways toward the desired one and hindering side product formation especially solid humins as the lagest challenge of this reaction. Several heterogeneous catalysts were studied in the literature for the related reactions such as resins, zeolites, metal oxides, mesoporous silica and organic polymers [30,31]. For instance, in a study by Tapas *et al*. ion-exchanged Sn-Beta zeolite was selected as a Lewis acid catalyst for isomerization of glucose to fructose and further transformations to LA. To achieve this goal a Brønsted acid catalyst had to be added giving with such dual solid-acid catalysts, 52% of levulinic acid yield from glucose [32]. Suacharoen *et al*. introduced alumina to SBA-15 by the post synthesis technique and obtained Al-SBA-15 as a catalyst with high Lewis acidity. This catalyst displayed a low activity resulting in 23% of LA yield. In addition, introduction of Ni or Ru to Al-SBA-15 only slightly improved the yields of LA [33]. Thus, presence of appropriate acidity and also the right balance of the Lewis and Brønsted acid sites are crucial.

Up to now, few studies were reported regarding post-synthesis grafting of SBA-15 to improve the Brønsted acid sites for carbohydrate conversion to 5-HMF [34–37]. The present work aims at the modification of SBA-15 for improving both Lewis and Brønsted acidity and attaining their proper balance to obtain a sustainable and versatile heterogenous catalyst for glucose conversion to LA.

2. Experimental Part

2.1 Catalyst preparation

SBA-15 synthesis

Mesoporous SBA-15 was synthesized according to Zhao *et al.* using TEOS (tetraethyl orthosilicate) as a silica source, P123 (EO_{20}-PO_{70}-EO_{20}) as a template in hydrochloric acid (pH<1) solution [38]. The mixture was continuously stirred for 20 h at 25 °C and crystallized in a Teflon autoclave at 90 °C for 24 h. The mixture was then filtered, washed, dried at 80 °C for 24 h and finally calcined in air (50 mL/min) at 500 °C for 6 h.

Introduction of alumina by evaporation-impregnation method

Alumina was introduced to SBA-15 by the evaporation impregnation method. Various amounts of $Al(NO_3)_3$*$9H_2O$ (Sigma-Aldrich), were dissolved in 250 mL of water, to prepare materials with SiO_2/Al_2O_3 ratios of 35, 32 and 30. After the complete dissolution of the salt, SBA-15 was added to the solution and stirred at 60 °C for 24 h. The mixtures were evaporated in vacuum at 60 °C. The obtained powders were calcined at 500 °C for 6 h. The final catalysts were labelled SBA-Al-EI-x, where x is the ratio between SiO_2 and Al_2O_3.

Introduction of sulfonic functionalities

A post-grafting method was used to functionalize selected SBA-15 materials. (3-mercaptopropyl)trimethoxysilane (MPTMS, 95 % Merck) was used as a grafting agent. 1 g of the SBA-Al-EI-32 was dissolved in 30 mL of saline (NaCl) solution. 0.2 M. MPTMS was added in the

appropriate molar ratio ($2SiO_2$: 1MPTMS) and stirred for 24 h at 90 °C. The solid was then washed in water and dried for 18 h at 70 °C. Thereafter, mild oxidation with 30 wt% H_2O_2 (molar ratio SiO_2:H_2O_2 = 2:0.11) was performed stirring for 24 h at 30 °C. The sulfonated solid was filtered, washed with methanol and dried at 25 °C for 18 h. The final catalyst was labelled SBA-Al-EI-32-SO_3H.

2.2. Characterization techniques

X-ray powder diffraction (XRD) analyses were carried out by a Bruker D8 Advance diffractometer equipped with a Si(Li) solid state detector (SOL-X) and a sealed tube providing Cu Kα radiation at an accelerated voltage of 40 kV and an applied current of 30 mA.

Scanning electron microscopy (Zeiss Leo Gemini 1530) was used to study the crystal morphology of the Al_2O_3-SBA-15 composites synthesized using evaporation impregnation method. Energy dispersive X-ray micro-analyses (EDX) attached to SEM was applied for quantitative elemental analyses.

Specific surface areas and pore size distributions were evaluated from N_2 adsorption/desorption isotherms at -196 °C using a Tristal II Plus Micromeritics. The surface areas were calculated using the BET method [39] whereas the pore size distribution was determined by the Barrett-Joyner-Halenda (BJH) method [40], applied to the N_2 desorption branch of the isotherm.

Transmission electron microscopy was used to study the structure, pore size and periodic porous order of the SBA mesoporous catalysts. The instrument applied for the measurements was JEM 1400 plus with an acceleration voltage of 120 kV and resolution of 0.98 nm using Quemsa II MPix bottom mounted digital camera. The particle size distribution was calculated with the aid of ImageJ software.

Characterization of the Brønsted and Lewis acid sites, their amount and strength were done using pyridine (Sigma Aldrich, ≥ 99.5%) adsorption-desorption. The measurements were performed with ATI Mattson FTIR using 10 mg of self-supported catalyst pellets. The catalyst was activated in the IR cell by heating from room temperature to 200 °C under vacuum (1×10^{-4} Pa). In order to

discriminate between weak, medium and strong acid sites, desorption of pyridine was performed at 150 °C, 250 °C and 350 °C, respectively. Pyridine was desorbed for 60 min at each temperature. Quantification of Brønsted and Lewis acid sites was done by considering intensity of IR signals at 1545 cm^{-1} and 1455 cm^{-1}, respectively, using the molar extinction factor given by Emeis [41].

2.3 Catalytic tests

The catalysts were tested in glucose hydrolysis in a stainless-steel autoclave (Parr Inc, USA). The temperature was measured with a thermocouple and automatically adjusted with an inbuilt temperature regulator (Parr4848 Reactor Controller). The autoclave was equipped with a gas inlet/sampling outlet fitted with 7 μm metal filter. Before the reaction, 500 mg of the substrate, 100 mL of water and 500 mg of the powdered catalyst were loaded into the reactor and then heated to 180 °C under 10 bar of N_2. The initial time of the reaction was taken once the reaction temperature was reached. The reaction was carried out for 7 hours at 1000 rpm to minimize mass transfer limitation. Throughout an experiment, the samples were taken at suitable intervals. At the end of the reaction, the mixture was cooled down to 25 °C and separated by filtration. The final reaction mixture and every samples were analysed by high performance liquid chromatography (HPLC) VWR HITACHI Chromaster, equipped by an Aminex HPX-87H column kept at 50 °C. 5450 RI detector was used for analytes identification and quantification.

Catalytic behaviour was evaluated in terms of conversion and the molar product yield:

$$Conversion\ (\%) = \frac{(mol\ substrate\ in) - (mol\ substrate\ at\ a\ certain\ time)}{mol\ substrate\ in} \cdot 100$$

$$Yield\ (\%) = \frac{mol\ i\ at\ a\ certain\ time}{mol\ substrate\ in} \cdot 100$$

Where *i* represents a particular reaction product.

3. Results and Discussion

3.1 Influence of alumina introduction

Small angle XRD patterns of the pristine SBA-15 and alumina incorporated ones with different SiO_2/Al_2O_3 ratios are presented in Figure 1.

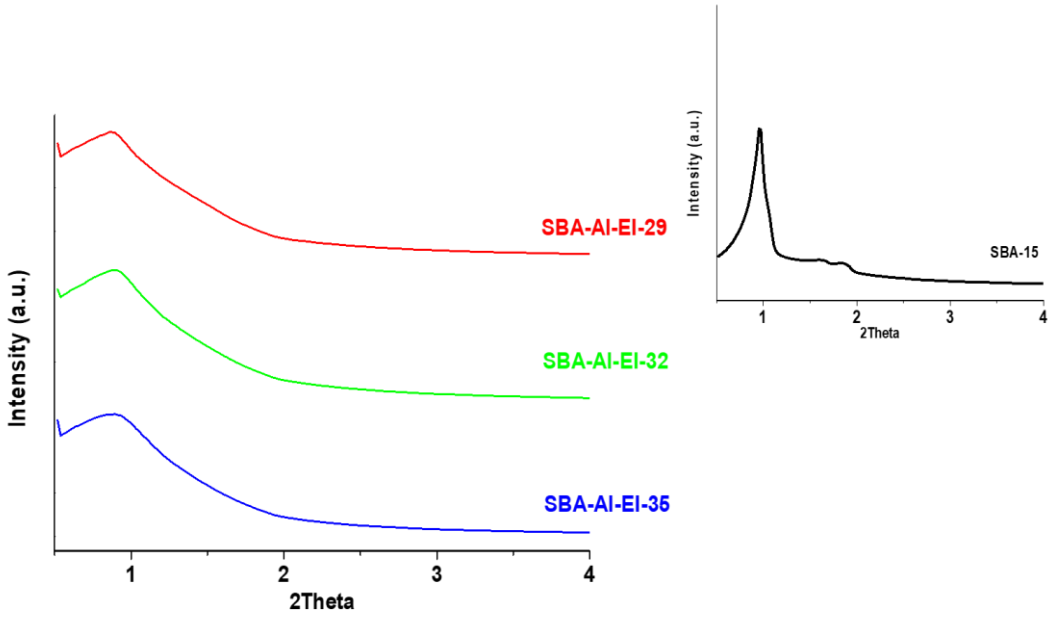

Figure 1. XRD patterns for pristine SBA-15 (in the in-set) and alumina modified samples.

Pristine SBA-15 exhibits three characteristic reflections at a low angle typical of ordered mesoporous materials with a 2D-hexagonal *p6mm* pore symmetry [42]. The peaks that appear at 0.95°, 1.64° and 1.85°, are associated with (100), (110) and (200) planes, respectively [43]. In the alumina-silica materials (SBA-Al-EI), a pronounced loss in the mesoporous order is evident reflected by a complete disappearance of the second and third peaks. Furthermore, the intensity of the reflection of the first main peak at 0.95° is attenuated in promoted samples. Another interesting aspect is the shift of the main peak to a lower angle (0.92°) in comparison with the pristine silica. This shift can be explained by the introduction of alumina in the framework diminishing the segment ordered hexagonal symmetry [44]. In addition, no significant difference in intensity can be noted in the catalysts with different SiO_2/Al_2O_3 ratios while a shift in the diffraction angle is perceptible. As reported by Xing

et al, when alumina is introduced inside the framework, there was a decrease in the segmental ordered hexagonal symmetry. In this case, no direct correlation between the alumina amount and the diffraction angle can be seen with the diffraction angles equal to 0.85°, 0.9° and 0.88° for SBA-Al-EI-29, SBA-Al-EI-32 and SBA-Al-EI-35, respectively [12]. At the same time, this small difference can be related to minor differences in speciation of alumina reflecting its location in or outside the framework.

The amount of alumina in the final catalysts was determined using SEM coupled with EDX; in this case, a direct correlation between the nominal and the actual loadings was observed as visible from Table 1. Figure 2 represents SEM images of alumina modified SBA-15 catalysts.

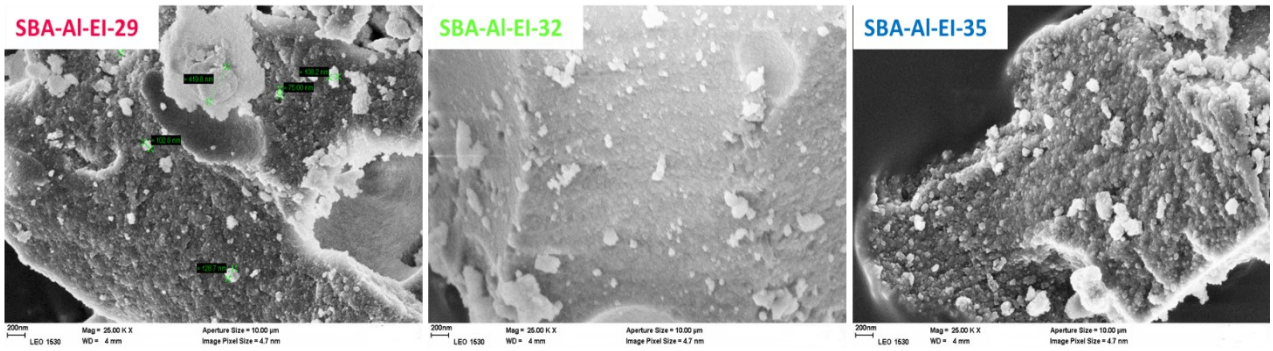

Figure 2 SEM images of SBA-Al-EI materials synthesized with different SiO_2/Al_2O_3 ratios

Table 1 Textural and structural properties of solid catalysts

Sample	S_{BET} (m^2/g)[a]	V_p (cm^3/g)[b]	d_p (nm)[c]	Si/Al[d]	SiO_2/Al_2O_3[e]
SBA-15	850	0.80	2-7.5	-	-
SBA-Al-EI-29	548	0.75	2-15	25	29
SBA-Al-EI-32	627	0.68	2-15	27	32
SBA-Al-EI-35	621	0.66	2-15	29	35

([a] Specific surface area, [b] Pore volume, [c] Average pore diameter, [d] silicon /aluminium ratios and [e] silica/alumina ratio)

As can be seen in Figure 2, SBA-Al-EI composites are made of spherical shaped particles (silica) and of larger *alumina* agglomerates characterized by a range of sizes and shapes.

N_2-physisorption was performed to evaluate the surface area, pore volume and pore size distributions of SBA-15 catalysts. The isotherms of the SBA-15 and SBA-Al-EI samples and the corresponding BJH pore size distributions are reported in Figure 3. All SBA-15 samples exhibit type IV isotherm curves with the characteristic hysteresis loop of mesoporous materials [45].

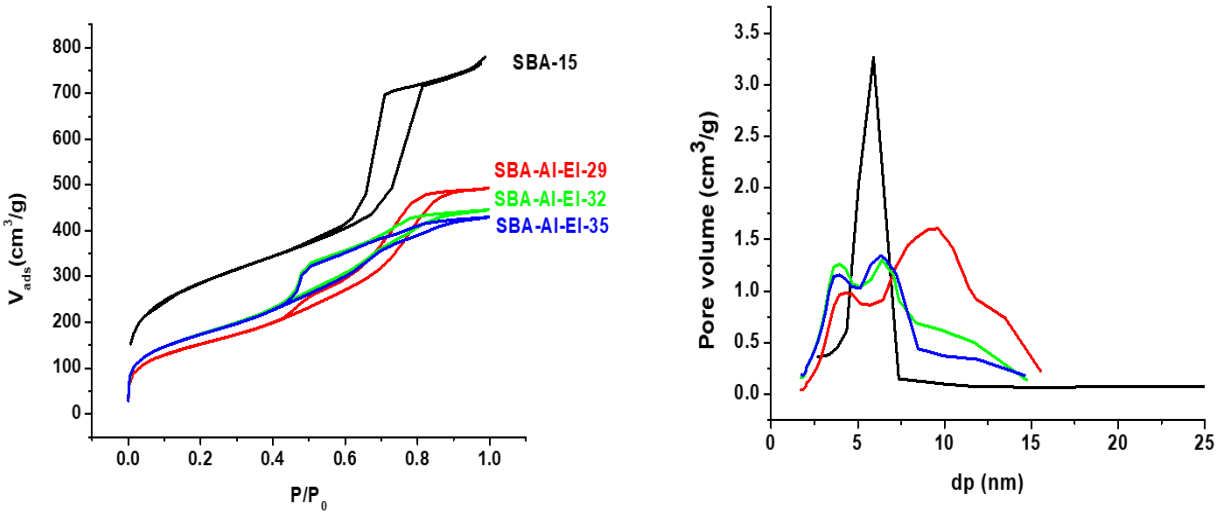

Figure 3. N_2 adsorption-desorption isotherms (a) and BJH pore size distribution (b) of SBA-15 and alumina/SBA-15 catalysts.

SBA-15 shows the H1 hysteresis shape with a sharp pore size distribution centred at 6 nm, characteristic of an ordered material with a bottle-necked pore opening [46]. For the modified samples, as already evidenced in the small-angle XRD patterns, the order is partially lost since the hysteresis shape is more irregular, with a wide and uneven distribution of the pore diameter. In SBA-Al-EI samples, the hysteresis loop, even if not easily classified, are characteristic of pores with non-homogeneous shape, being centred between the P/P_0 of 0.4 and 0.8 with a broad distribution. Indeed, looking at the data reported in Table 1, alumina evaporation-impregnation technique seems to strongly affect the surface area, leading to a decrease of almost 200-300 m^2/g from the pristine catalyst. The decrease in the surface area can be attributed to the pore blockage of SBA-15 with Al_2O_3 nanoparticles during modification using the evaporation impregnation method. Regarding alumina modified samples with different SiO_2/Al_2O_3 ratios, SBA-Al-EI-32 and SBA-Al-EI-35 are more

similar to each other than SBA-Al-EI-29. As can be seen, the hysteresis curves are almost overlapping. Moreover, SBA-Al-EI-29, having the highest alumina content, exhibits the lowest surface area (Table 1). In this case, such marked differences can be attributed not only to a higher amount of alumina but also to its position inside/outside the silica lattice. The plausible explanation for such low surface area for SBA-15-Al-29 mesoporous catalyst is the blocking of pores with large nanoparticles of Al_2O_3, furthermore, such decrease in surface can also be combined with the partial loss of the mesoporous order. The surface area alteration after incorporation of alumina is in agreement with the results reported in the literature [13,47].

Transmission electron microscopy (TEM) was used for investigation of the morphology of SBA-15 mesoporous materials prepared using the evaporation impregnation method. Transmission electron micrographs of SBA-Al-EI samples are reported in Figure 4, together with the image of the pristine SBA-15, illustrating that the ordered mesoporous material is characterised by random 2-D hexagonal mesostructures. Such effect on the structure is in good agreement with small-angle XRD patterns and N_2-physisorption. Moreover, in the TEM image, alumina agglomerates are clearly visible; small and homogeneously dispersed in SBA-Al-EI, in line with SEM. Hence, a proper distribution of alumina agglomerates on the SBA-15 framework with a partial impact on the mesoporous order was obtained for the composite prepared by the evaporation-impregnation method. At higher Al content, the order decreased or was even completely lost. In general, this led to agglomeration of Al species on the surface that resemble to some extent the materials synthesized by groups of Hensen and Su [44,48].

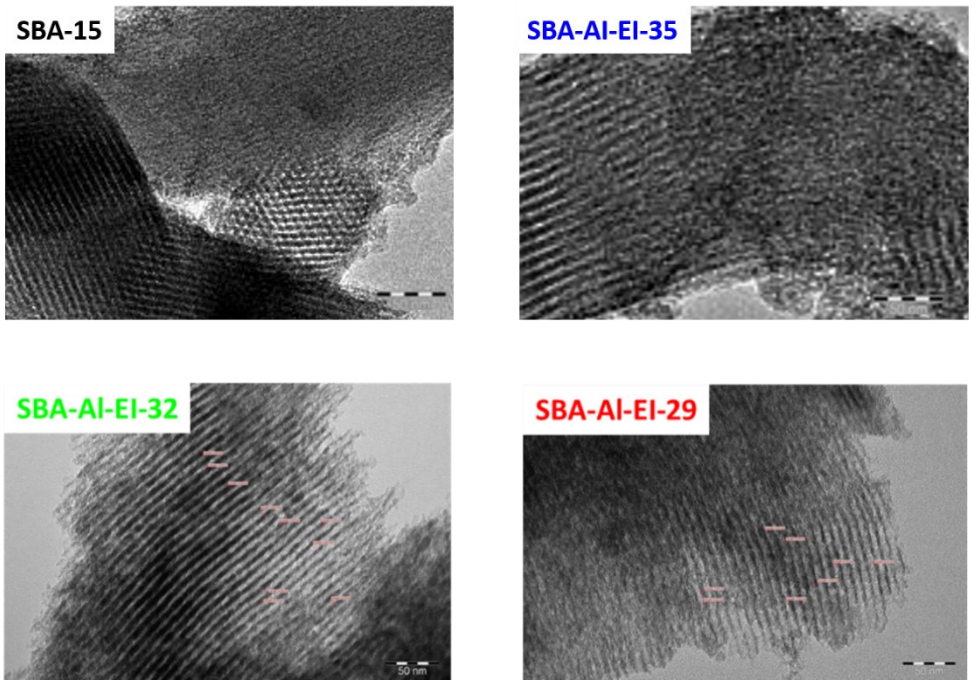

Figure 4 TEM images of pristine SBA15 and of different SiO_2/Al_2O_3 evaporation-impregnation catalysts

Table 2 summarises the concentration and the types of acid sites, determined by FTIR spectroscopy of pyridine adsorption in the spectrum range of 1400-1575 cm^{-1}. For each catalyst, the concentration of Brønsted and Lewis acid sites at different temperatures is given. Values at higher temperature reflect sites with stronger acidity [49].

Table 2. Concentration of Brønsted acid sites (B) and Lewis acid sites (L) in the alumina modified SBA-15 with different SiO_2/Al_2O_3 ratios determined with FTIR-pyridine method. Concentration expressed in µmol/g

	SBA-Al-EI-29			SBA-Al-EI-32			SBA-Al-EI-35		
T (°C)	C_B	C_L	Total	C_B	C_L	Total	C_B	C_L	Total
150	19	33	52	26	44	70	27	74	101
250	10	19	29	17	24	41	16	17	33
350	0	0	0	0	4	4	0	2	2

Unmodified SBA-15 did not show any peaks originating from pyridine adsorbed on acid sites. As reported in Table 2, the catalyst with the highest amount of alumina (SBA-Al-EI-29) has the lowest

number of sites at each temperature, with no strong sites desorbing pyridine at 350 °C. This can be related to loading of Al which has a large influence on alumina dispersion of alumina on the SBA-15 surface. SBA-Al-EI-29 with the highest alumina loading led to a low alumina dispersion and thus a low accessibility of Lewis acid sites which caused a lower number of Lewis acid sites according to FTIR-pyridine analysis [10]. SBA-Al-EI-32 and SBA-Al-EI-35, unlike SBA-Al-EI-29, have shown strong Lewis acid sites. Particularly, SBA-AL-EI-32 has shown the highest concentration of medium and strong Lewis acid sites at 250 and 350 °C, respectively. For all catalysts, no strong Brønsted acid sites are present. Typically as the aluminium content increases, the amount of sites increases at the expense of its strength [50]. This was not in agreement with the obtained results because a higher amount of medium and strong acid sites was found in the sample with the intermediate amount of alumina. Even in this case, it can be hypothesised that the effect is strongly connected with alumina speciation.

In summary the aluminium amount even in a narrow range influences morphological and structural property of the final materials. The catalyst with the highest amount of alumina SBA-Al-EI-29 exhibits properties the most different from the rest of the materials. It has the lowest surface area with a different hysteresis shape and the lowest amount of acid sites. Considering the other two samples, only slight changes in the properties were observed. Among them, the most important feature is the presence of strong Lewis acid sites in the intermediate alumina sample SBA-Al-EI-32. Contrary to expectations, the most acidic samples had the lowest aluminium content. This is probably due to the coordination of the aluminium ion. Therefore, determination of Al coordination in the studied materials was performed using ^{27}Al-NMR (Figure 5).

a)

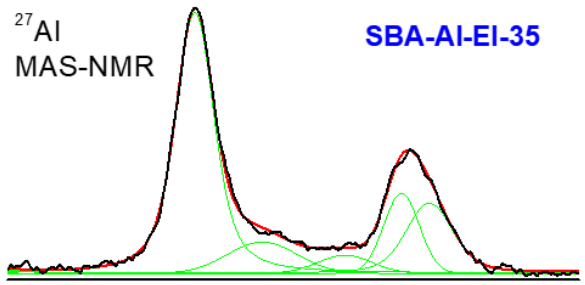

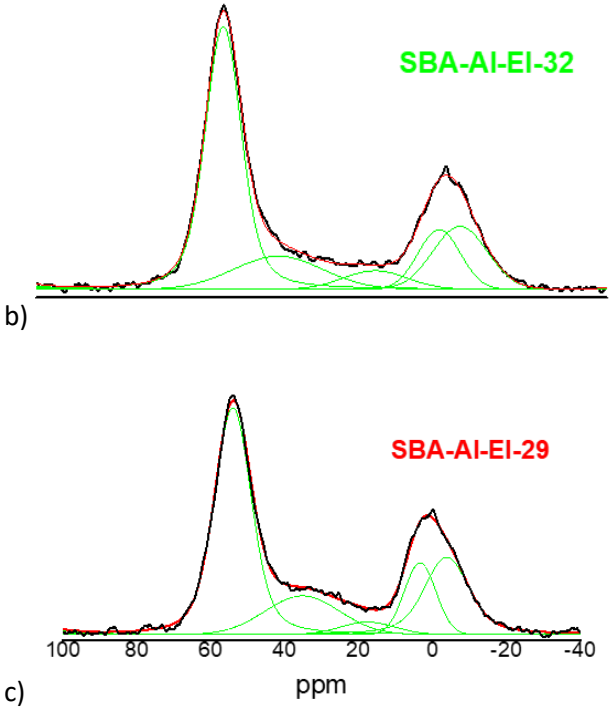

Figure 5 ^{27}Al MAS-NMR spectra of catalysts with different Si/Al ratios.

Each spectrum was decomposed by five Gaussian lines. For three samples, the most significant peak is around 54 ppm which is typical for tetrahedral coordinated AlO_4 groups. A broad line around 35 to 40 ppm and the broad weak line at 17 ppm can be assigned to 5- coordinated Al sites. The resonance at 3 and 4 ppm belong to octahedral 6 coordinated Al sites [51,52].

Table 3 Relative contribution of different forms of Al calculated from ^{27}Al-NMR

	^{27} Al-NMR		
Samples	Al (IV) %	Al (V) %	Al (VI) %
SBA-Al-EI-29	49.3	18.2	32.5
SBA-Al-EI-32	52.6	19.5	27.9
SBA-Al-EI-35	55.7	14.3	30

Table 3 summarises the relative contribution of different forms of Al. It can be noted that the relative number of tetrahedral Al (IV) sites gradually increases with decreasing the Al content at the expense

of the extra-framework Al (V) and Al (VI) sites. Nevertheless, the distribution of Al (V) and Al (VI) does not follow the same trend. Indeed, SBA-Al-EI-32 with the intermediate silica to alumina ratio among the tested materials has the lowest amount of the extra-framework octahedral Al sites [50]. Moreover, the total number of Al sites is varying as 107:93:100 for SBA-Al-EI-29: SBA-Al-EI-32: SBA-Al-EI-35, respectively. Subsequently, the material with the highest number of strong and medium acid sites is the one with the lowest octahedral Al and the lowest total number of sites. As was reported in N_2-physisorption results, SBA-Al-EI-32 had the lowest surface area decrease and pore broadening after modification with respect to the other samples. Hence, a combination of several factors such as the appropriate amount of introduced alumina, the lowest extra-framework octahedral Al, desirable framework tetrahedral Al and larger surface area and pore size distribution of SBA-Al-EI-32 was beneficial in achieving the highest amount of strong Lewis acid sites and their better accessibility for the reactants.

3.3. Reactivity

Silica-alumina materials with different SiO_2/Al_2O_3 ratios were tested in the glucose hydrolysis. Glucose conversion is reported in Figure 6 while Figure 7 displays yields of 5-HMF and levulinic acid as a function of time.

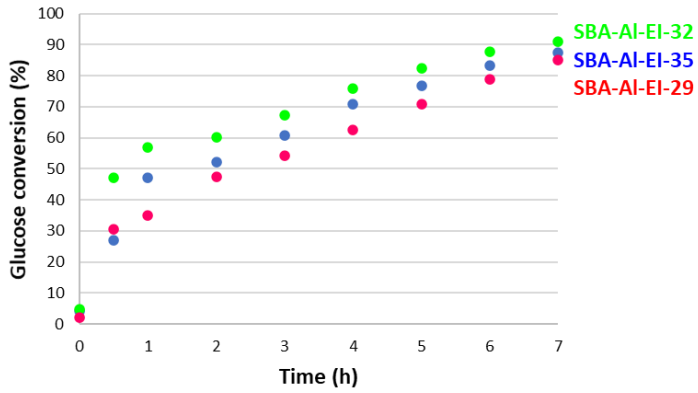

Figure 6. Glucose conversion as a function of time in hydrolysis of glucose for catalysts with different SiO_2/Al_2O_3 ratios. Reaction conditions: 180 °C, 2.7 mmol glucose, 500 mg catalyst, 100 mL H_2O.

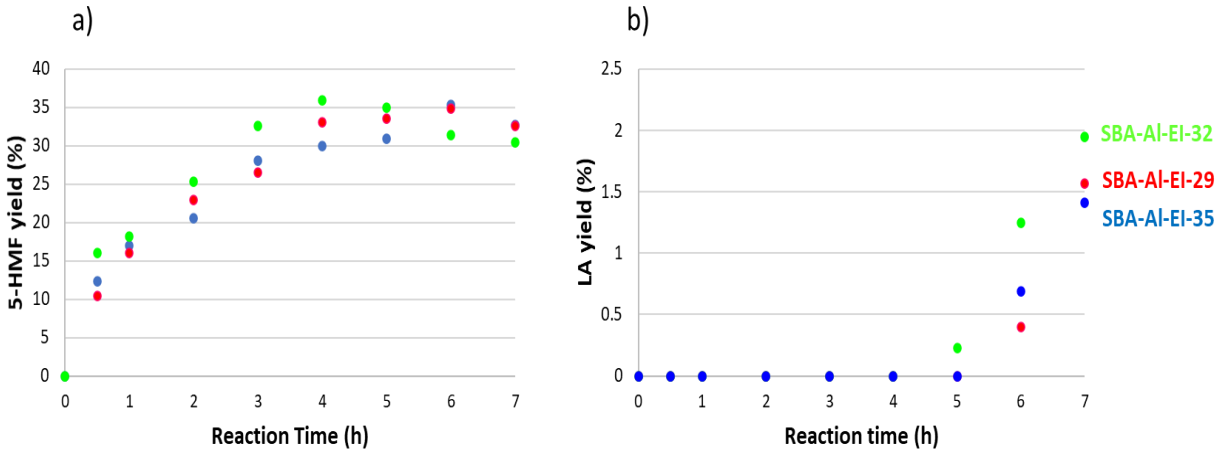

Figure 7. Yields of products as a function of time in hydrolysis of glucose for catalysts with different SiO_2/Al_2O_3 ratios: a) 5-HMF, b) levulinic acid (LA). Reaction conditions: 180 °C, 2.7 mmol glucose, 500 mg catalyst, 100 mL H_2O.

Considering glucose conversion, three catalysts exhibited similar profiles with a high consumption rate in the first hour declining thereafter. SBA-Al-EI-32 exhibited almost 60 % of conversion after one hour, reaching 90 % after 7 hours. The corresponding values for other catalysts were similar, moreover the slopes in conversion vs time dependences were also rather similar after the initial

period. The concentration profiles of 5-HMF and LA (Figure 7) clearly indicate consecutive reactions with 5-HMF being the intermediate of C6-sugar transformations. This intermediate is subsequently rehydrated to give levulinic acid and formic acid [53]. Since the pristine silica mesoporous materials are not active for the latter reaction due to the lack of acid sites, some studies were reported regarding incorporation of aluminium in the silica framework by different synthesis methods. However, aluminium or alumina introduction only guarantees Lewis acidity improvement and can catalyse a part of the reaction pathway until the production of 5-HMF as the intermediate of the reaction [54,55] as also reported in the current work. The latter reaction requires Brønsted acid sites, while isomerization of glucose to fructose followed by dehydration to 5-HMF occurs on Lewis acid sites [56]. A small amount of weak and medium Brønsted acid sites with no strong sites present in the catalysts is apparently a reason for low yields of levulinic acid.

Among the tested materials SBA-Al-EI-32 gave the slightly highest glucose conversion, and LA yields possessing the highest concentration of Lewis acid sites of medium and strong strength [57]. Low yield of levulinic acid calls for further modification of this promising material.

3.4. Incorporation of Brønsted acid sites

Introduction of Brønsted acid sites was achieved using post-synthesis grafting method as detailed in the Experimental part, following the previous work of Pizzolitto *et al*, [36] The obtained material, SBA-Al-EI-32-SO_3H, was fully characterized via N_2-physisorption, TEM, small-angle XRD and SEM-EDX (Figure 8).

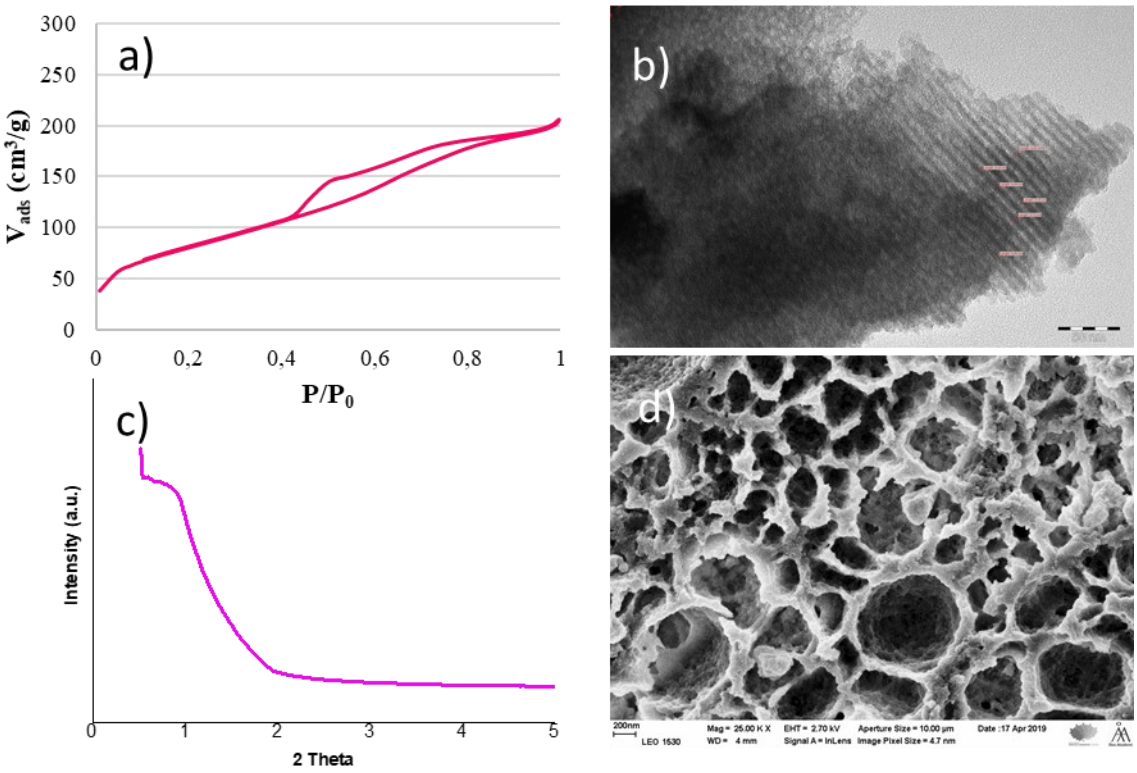

Figure 8. Characterisation of SBA-Al-EI-32-SO_3H: a) N_2-physisorption, b) TEM, c) low-angle XRD and d) SEM.

Characterization data clearly confirm that grafting strongly affects morphological and structural features of the material. The surface area has drastically decreased from 627 to 294 m^2/g and the SEM image (Figure 8d) appears to be completely different from the not-grafted one. In the literature there are conflicting reports for similar materials after grafting. For instance, Hermida *et al.,* obtained a sulfonic acid functionalized SBA-15 after post-synthesis with a higher mesoporous surface area and almost similar fibrous and porous-type morphology with respect to the parent SBA-15 [58]. Pirez *et al*. suggested that since the surface of silica is sensitive, a mild hydrothermal treatment should be used to keep the surface and morphology of the grafted sample intact. Similar to the current work, the saline (NaCl) solution with a different ratio was used as the grafting solvent with XRD and TEM showing that grafted SBA-15 retained its mesoporous structure and morphology [59]. Sasidharan *et al* has demonstrated a slight decrease of the SBA-15 pore volume and the surface area after grafting compared to the parent one [60]. However, no work was found about post grafting of Al-SBA-15,

and in the current work, completely different properties were obtained after grafting compared to the pristine SBA-15.

Nevertheless, a partial order and the mesoporous structure of the parent material were still preserved. Acidity data based on FT-IR spectroscopy with pyridine as a probe molecule are shown in Table 4.

Table 4. Concentration of Brønsted acid sites (B) and Lewis acid sites (L) in SBA-Al-EI-32-SO_3H determined by FTIR with pyridine.

	C_B (μmol/g)	C_L(μmol/g)	Total (μmol/g)
150 °C	233	15	248
250 °C	59	5	64
350 °C	7	0	7

SBA-Al-EI-32-SO_3H, in comparison with SBA-Al-EI-32 (Table 2), shows a higher concentration of weak, medium and strong Brønsted acid sites, indicating effectiveness of the grafting approach. Catalytic behaviour of the grafted material in glucose hydrolysis is reported in Figure 9, where for comparison the data for the parent material are also presented.

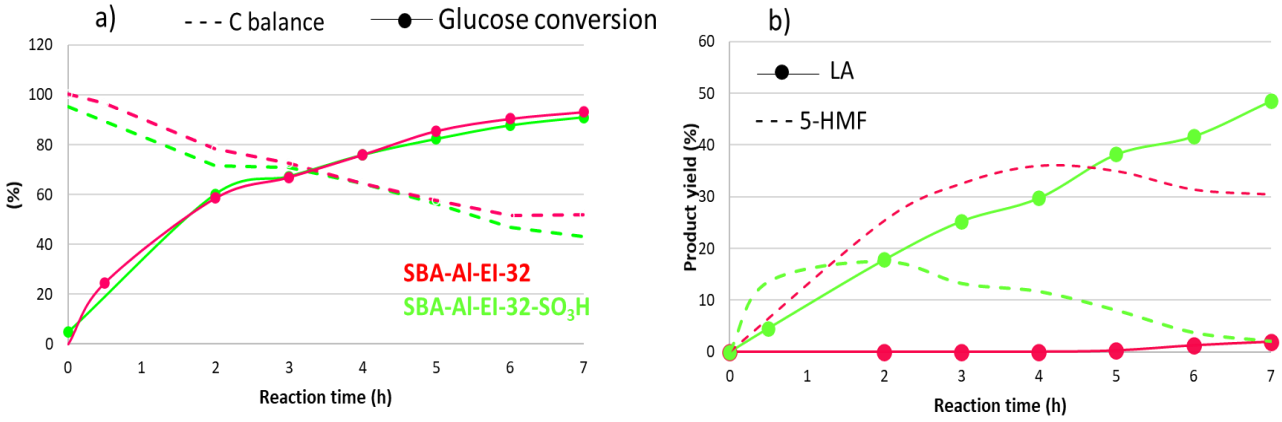

Figure 9. Glucose hydrolysis over SBA-Al-EI-32 and SBA-Al-EI-32-SO_3H catalysts: a) conversion, b) products yield. Reaction conditions: 180 °C, 2.7 mmol glucose, 500 mg catalyst, 100 mL H_2O.

As it can be seen from Figure 9a, there are no substantial differences in conversion and carbon balance, while the yields of LA were significantly different, namely introduction of the sulfonic

groups led to an increase in the LA yield from 2% to 50 % during seven hours of the reaction. In the literature, some studies were found in which the effect of post synthesis alumina introduction or sulfonic group grafting were investigated and due to the lack of Lewis or Brønsted acid sites and their balance, only a shorter reaction pathway was catalysed or a low product yield was attained. For instance, Crisci *et al* used SBA-15 post grafted with several sulfonic functionalities giving the catalysts rich in Brønsted acid sides which were effective in conversion of fructose to 5-HMF [37]. On the other hand, Suacharoen *et al* incorporated alumina as Lewis acid sites to SBA-15 by the post synthesis method and were able to obtain only a low yield of LA from glucose [61]. Therefore, the presence of both Lewis and Brønsted acid sites is of crucial importance in order to achieve a higher yield of LA as the desired product. High activity of SBA-Al-EI-32-SO_3H as the best catalyst of this study is due to both acid functionalities introduced to SBA-15.

4. Conclusions

In this work, the formulation of an acid heterogeneous catalyst based on SBA-15 was successfully performed. For the first time, both Brønsted and Lewis acid sites were successfully introduced into SBA-15. In particular, post synthesis optimization of mesoporous material was carried out to attain a compromise and synergy among the surface area, pore dimension and balanced acidity. Introduction of alumina to SBA-15 using the evaporation impregnation method led to the improvement of medium and strong Lewis acid sites accompanied by a partial maintenance of the pore order and simultaneous retention of the surface area and large pores. Then, introduction of sulfonic acid groups using the post-synthesis grafting method boosted Brønsted acidity of SBA-15. This type of acid modified silica alumina-based materials can be efficient in sugars and other biomass transformations possessing several key factors such as pore accessibility, and fine-tuned acidity, allowing these desired selectivity and activity.

References

[1] C. Sci, J.G. De Vries, S.D. Jackson, Homogeneous and heterogeneous catalysis in industry, (2012) 4443. https://doi.org/10.1039/c2cy90039d.

[2] A. Heras, M.B. Gu, A. Iriondo, J.F. Cambra, Levulinic Acid Production Using Solid-Acid Catalysis Ilian Guzma n, (2016). https://doi.org/10.1021/acs.iecr.5b04190.

[3] B. Agarwal, K. Kailasam, R.S. Sangwan, S. Elumalai, Traversing the history of solid catalysts for heterogeneous synthesis of 5-hydroxymethylfurfural from carbohydrate sugars: A review, Renewable and Sustainable Energy Reviews. 82 (2018) 2408–2425. https://doi.org/10.1016/j.rser.2017.08.088.

[4] Y. Zhang, Q. Xiong, E. Zhu, M. Liu, J. Pan, Y. Yan, Direct Conversion of C6 Monosaccharide-Based Carbohydrates to 5-Hydroxymethylfurfural by the Combination of Sulfated Zirconia and Ceria Catalysts, Energy Technology. 6 (2018) 1941–1950. https://doi.org/10.1002/ente.201800052.

[5] H. Schepers, J. Geboers, P.A. Jacobs, B. Goderis, S. Van de Vyver, C.J. Gommes, B.F. Sels, L. Peng, F. de Clippel, Sulfonated silica/carbon nanocomposites as novel catalysts for hydrolysis of cellulose to glucose, Green Chemistry. 12 (2010) 1560. https://doi.org/10.1039/c0gc00235f.

[6] N.A.S. Ramli, N.A.S. Amin, Fe/HY zeolite as an effective catalyst for levulinic acid production from glucose: Characterization and catalytic performance, Applied Catalysis B: Environmental. 163 (2015) 487–498. https://doi.org/10.1016/j.apcatb.2014.08.031.

[7] X. Li, R. Xu, Q. Liu, M. Liang, J. Yang, S. Lu, G. Li, L. Lu, C. Si, Industrial Crops & Products Valorization of corn stover into furfural and levulinic acid over SAPO-18 zeolites : Effect of Brønsted to Lewis acid sites ratios, Industrial Crops & Products. 141 (2019) 111759. https://doi.org/10.1016/j.indcrop.2019.111759.

[8] M. Choi, W. Heo, F. Kleitz, R. Ryoo, Facile synthesis of high quality mesoporous SBA-15 with enhanced control of the porous network connectivity and wall thicknessElectronic

supplementary information (ESI) available: structural parameters (Table 1) and N2 adsorption?desorption isotherms at 7, Chemical Communications. 75 (2003) 1340. https://doi.org/10.1039/b303696k.

[9] Z.Y. Wu, H.J. Wang, T.T. Zhuang, L.B. Sun, Y.M. Wang, J.H. Zhu, Multiple functionalization of mesoporous silica in one-pot: Direct synthesis of aluminum-containing plugged SBA-15 from aqueous nitrate solutions, Advanced Functional Materials. (2008). https://doi.org/10.1002/adfm.200700706.

[10] B. Kilos, I. Nowak, M. Ziolek, A. Tuel, J.C. Volta, Transition metal containing (Nb, V, Mo) SBA-15 molecular sieves - Synthesis, characteristic and catalytic activity in gas and liquid phase oxidation, Studies in Surface Science and Catalysis. 158 B (2005) 1461–1468. https://doi.org/10.1016/s0167-2991(05)80498-7.

[11] K. Szczodrowski, B. Prélot, S. Lantenois, J.M. Douillard, J. Zajac, Effect of heteroatom doping on surface acidity and hydrophilicity of Al, Ti, Zr-doped mesoporous SBA-15, Microporous and Mesoporous Materials. 124 (2009) 84–93. https://doi.org/10.1016/j.micromeso.2009.04.035.

[12] S. Xing, P. Lv, J. Fu, J. Wang, P. Fan, Microporous and Mesoporous Materials Direct synthesis and characterization of pore-broadened Al-SBA-15, Microporous and Mesoporous Materials. 239 (2017) 316–327. https://doi.org/10.1016/j.micromeso.2016.10.018.

[13] E. Ghedini, M. Signoretto, F. Pinna, G. Cruciani, Mesoporous silica-zirconia systems for catalytic applications, Catalysis Letters. 125 (2008) 359–370. https://doi.org/10.1007/s10562-008-9459-8.

[14] I.K. Mbaraka, B.H. Shanks, Design of multifunctionalized mesoporous silicas for esterification of fatty acid, Journal of Catalysis. 229 (2005) 365–373. https://doi.org/10.1016/j.jcat.2004.11.008.

[15] X. Wang, C.C. Chen, S.Y. Chen, Y. Mou, S. Cheng, Arenesulfonic acid functionalized mesoporous silica as a novel acid catalyst for the liquid phase Beckmann rearrangement of

cyclohexanone oxime to E-caprolactam, Applied Catalysis A: General. 281 (2005) 47–54. https://doi.org/10.1016/j.apcata.2004.11.011.

[16] L. Zhou, Z. Liu, M. Shi, S. Du, Y. Su, X. Yang, J. Xu, Sulfonated hierarchical H-USY zeolite for efficient hydrolysis of hemicellulose/cellulose, Carbohydrate Polymers. 98 (2013) 146–151. https://doi.org/10.1016/j.carbpol.2013.05.074.

[17] C. Pirez, J.M. Caderon, J.P. Dacquin, A.F. Lee, K. Wilson, Tunable KIT-6 mesoporous sulfonic acid catalysts for fatty acid esterification, ACS Catalysis. (2012). https://doi.org/10.1021/cs300161a.

[18] C. Pirez, M. Tapia Reche, A.F. Lee, J.C. Manayil, V.C. Dos-Santos, K. Wilson, Hydrothermal Saline Promoted Grafting of Periodic Mesoporous Organic Sulfonic Acid Silicas for Sustainable FAME Production, Catalysis Letters. 145 (2015) 1483–1490. https://doi.org/10.1007/s10562-015-1559-7.

[19] J. Cheng, Z. Zhang, X. Zhang, J. Liu, J. Zhou, K. Cen, Sulfonated mesoporous Y zeolite with nickel to catalyze hydrocracking of microalgae biodiesel into jet fuel range hydrocarbons, International Journal of Hydrogen Energy. 44 (2019) 1650–1658. https://doi.org/10.1016/j.ijhydene.2018.11.110.

[20] X. Li, R. Xu, J. Yang, S. Nie, D. Liu, Y. Liu, C. Si, Production of 5-hydroxymethylfurfural and levulinic acid from lignocellulosic biomass and catalytic upgradation, Industrial Crops and Products. 130 (2019) 184–197. https://doi.org/10.1016/j.indcrop.2018.12.082.

[21] S.S. Chen, I.K.M. Yu, D.C.W. Tsang, A.C.K. Yip, E. Khan, L. Wang, Y.S. Ok, C.S. Poon, Valorization of cellulosic food waste into levulinic acid catalyzed by heterogeneous BrØnsted acids: Temperature and solvent effects, Chemical Engineering Journal. 327 (2017) 328–335. https://doi.org/10.1016/j.cej.2017.06.108.

[22] A. Corma Canos, S. Iborra, A. Velty, Chemical routes for the transformation of biomass into chemicals, Chemical Reviews. (2007). https://doi.org/10.1021/cr050989d.

[23] T. Werpy, G. Petersen, Top Value Added Chemicals from Biomass: Volume I -- Results of

Screening for Potential Candidates from Sugars and Synthesis Gas. Office of Scientific and Technical Information (OSTI), Office of Scientific and Technical Information. (2004) 69. https://doi.org/10.2172/15008859.

[24] J. He, H. Li, Y. Xu, S. Yang, Dual acidic mesoporous KIT silicates enable one-pot production of γ-valerolactone from biomass derivatives via cascade reactions, Renewable Energy. 146 (2020) 359–370. https://doi.org/10.1016/j.renene.2019.06.105.

[25] M. Signoretto, S. Taghavi, E. Ghedini, F. Menegazzo, Catalytic Production of Levulinic Acid (LA) from Actual Biomass, Molecules (Basel, Switzerland). 24 (2019) 1–20. https://doi.org/10.3390/molecules24152760.

[26] X. Li, K. Peng, Q. Xia, X. Liu, Y. Wang, Efficient conversion of cellulose into 5-hydroxymethylfurfural over niobia/carbon composites, Chemical Engineering Journal. 332 (2018) 528–536. https://doi.org/10.1016/j.cej.2017.06.105.

[27] J. Ahlkvist, J. Wärnå, T. Salmi, J.P. Mikkola, Heterogeneously catalyzed conversion of nordic pulp to levulinic and formic acids, Reaction Kinetics, Mechanisms and Catalysis. (2016). https://doi.org/10.1007/s11144-016-1069-7.

[28] S.S. Chen, T. Maneerung, D.C.W. Tsang, Y.S. Ok, C.H. Wang, Valorization of biomass to hydroxymethylfurfural, levulinic acid, and fatty acid methyl ester by heterogeneous catalysts, Chemical Engineering Journal. 328 (2017) 246–273. https://doi.org/10.1016/j.cej.2017.07.020.

[29] W. Weiqi, W. Shubin, Experimental and kinetic study of glucose conversion to levulinic acid catalyzed by synergy of Lewis and Brønsted acids, Chemical Engineering Journal. 307 (2017) 389–398. https://doi.org/10.1016/j.cej.2016.08.099.

[30] E. Lam, J.H.T. Luong, Carbon Materials as Catalyst Supports and Catalysts in the Transformation of Biomass to Fuels and Chemicals, (2014). https://doi.org/10.1021/cs5008393.

[31] S. Kang, J. Fu, G. Zhang, From lignocellulosic biomass to levulinic acid: A review on acid-

catalyzed hydrolysis, Renewable and Sustainable Energy Reviews. 94 (2018) 340–362. https://doi.org/10.1016/j.rser.2018.06.016.

[32] P. Parthasarathy, S.K. Narayanan, Effect of Hydrothermal Carbonization Reaction Parameters on, Environmental Progress & Sustainable Energy. 33 (2014) 676–680. https://doi.org/10.1002/ep.

[33] S. Suacharoen, D.N. Tungasmita, Hydrothermolysis of carbohydrates to levulinic acid using metal supported on porous aluminosilicate, Journal of Chemical Technology and Biotechnology. 88 (2013) 1538–1544. https://doi.org/10.1002/jctb.4000.

[34] K. Peng, X. Li, X. Liu, Y. Wang, Hydrothermally stable Nb-SBA-15 catalysts applied in carbohydrate conversion to 5-hydroxymethyl furfural, Molecular Catalysis. 441 (2017) 72–80. https://doi.org/10.1016/j.mcat.2017.04.034.

[35] C. Thunyaratchatanon, W. Sinsakullert, A. Luengnaruemitchai, 5-Hydroxymethylfurfural production from hexose sugars using adjustable acid- and base-functionalized mesoporous SBA-15 catalysts in aqueous media, (2019).

[36] C. Pizzolitto, E. Ghedini, F. Menegazzo, M. Signoretto, A. Giordana, G. Cerrato, G. Cruciani, E ff ect of grafting solvent in the optimisation of Sba-15 acidity for levulinIc acid production, Catalysis Today. 345 (2020) 183–189. https://doi.org/10.1016/j.cattod.2019.11.012.

[37] A.J. Crisci, M.H. Tucker, M. Lee, S.G. Jang, J.A. Dumesic, S.L. Scott, Acid-Functionalized SBA-15-Type Silica Catalysts for Carbohydrate Dehydration, (2011) 719–728. https://doi.org/10.1021/cs2001237.

[38] D. Zhao, Q. Huo, J. Feng, B.F. Chmelka, G.D. Stucky, Nonionic triblock and star diblock copolymer and oligomeric sufactant syntheses of highly ordered, hydrothermally stable, mesoporous silica structures, Journal of the American Chemical Society. 120 (1998) 6024–6036. https://doi.org/10.1021/ja974025i.

[39] S. Macko, P. H. E. Emmett, Brunauer, S., Emmett, P. H. & Teller, E. Adsorption of gases in

multimolecular layers. J. Am. Chem. Soc. 60, 309-319, 1938. https://doi.org/10.1021/ja01269a023.

[40] I. Union, O.F. Pure, A. Chemistry, INTERNATIONAL UNION OF PURE COMMISSION ON COLLOID AND SURFACE CHEMISTRY INCLUDING CATALYSIS * REPORTING PHYSISORPTION DATA FOR GAS / SOLID SYSTEMS with Special Reference to the Determination of Surface Area and Porosity, 57 (1985) 603–619.

[41] C.A. Emeis, Determination of integrated molar extinction coefficients for infrared absorption bands of pyridine adsorbed on solid acid catalysts, Journal of Catalysis. (1993). https://doi.org/10.1006/jcat.1993.1145.

[42] Z. Yang, W. Cai, J. Chou, Z. Cai, W. Jin, J. Chen, Z. Xiong, X. Ru, Q. Xia, Hydrothermal synthesis of plugged micro/mesoporous Al-SBA-15 from spent fluid catalytic cracking catalyst, Materials Chemistry and Physics. 222 (2019) 227–229. https://doi.org/10.1016/j.matchemphys.2018.10.026.

[43] D. Margolese, J.A. Melero, S.C. Christiansen, B.F. Chmelka, G.D. Stucky, Direct syntheses of ordered SBA-15 mesoporous silica containing sulfonic acid groups, Chemistry of Materials. 12 (2000) 2448–2459. https://doi.org/10.1021/cm0010304.

[44] A.J.J. Koekkoek, J.A.R. Van Veen, P.B. Gerrtisen, P. Giltay, P.C.M.M. Magusin, E.J.M. Hensen, Brønsted acidity of Al/SBA-15, Microporous and Mesoporous Materials. 151 (2012) 34–43. https://doi.org/10.1016/j.micromeso.2011.11.019.

[45] V. Meynen, P. Cool, E.F. Vansant, Verified syntheses of mesoporous materials, Microporous and Mesoporous Materials. 125 (2009) 170–223. https://doi.org/10.1016/j.micromeso.2009.03.046.

[46] E.M. Johansson, A. Galarneau, H. Cambon, F. Di Renzo, R. Ryoo, M. Choi, F. Fajula, D. Zhao, J. Sun, Q. Li, G.D. Stucky, S. Barbara, R. van Grieken, J.M. Escola, J. Moreno, R. Rodríguez, J. Xu, T. Chen, J.-K. Shang, K.-Z. Long, Y.-X. Li, J. Wang, H. Ge, W. Bao, E.M. Björk, D. Zhang, A. Duan, Z. Zhao, X. Wang, G. Jiang, J. Liu, C. Wang, M. Jin, M. Kruk,

M. Jaroniec, C.H. Ko, R. Ryoo, Controlling the Pore Size and Morphology of Mesoporous Silica, New Journal of Chemistry. (2015). https://doi.org/10.1016/j.cej.2009.07.016.

[47] E. Ghedini, M. Signoretto, F. Pinna, G. Cerrato, C. Morterra, Gas and liquid phase reactions on MCM-41/SZ catalysts, Applied Catalysis B: Environmental. 67 (2006) 24–33. https://doi.org/10.1016/j.apcatb.2006.04.010.

[48] X.Y. Yang, A. Vantomme, A. Lemaire, F.S. Xiao, B.L. Su, A highly ordered mesoporous aluminosilicate, CMI-10, with a Si/Al ratio of one, Advanced Materials. 18 (2006) 2117–2122. https://doi.org/10.1002/adma.200600247.

[49] A.A. Gurinov, Y.A. Rozhkova, A. Zukal, J. Čejka, I.G. Shenderovich, Mutable lewis and brønsted acidity of aluminated SBA-15 as revealed by NMR of adsorbed pyridine- 15N, Langmuir. 27 (2011) 12115–12123. https://doi.org/10.1021/la2017566.

[50] B. Dragoi, E. Dumitriu, C. Guimon, A. Auroux, Acidic and adsorptive properties of SBA-15 modified by aluminum incorporation, Microporous and Mesoporous Materials. 121 (2009) 7–17. https://doi.org/10.1016/j.micromeso.2008.12.023.

[51] Y. Li, W. Zhang, L. Zhang, Q. Yang, Z. Wei, Z. Feng, C. Li, Direct synthesis of Al-SBA-15 mesoporous materials via hydrolysis-controlled approach, Journal of Physical Chemistry B. 108 (2004) 9739–9744. https://doi.org/10.1021/jp049824j.

[52] W. Hu, Q. Luo, Y. Su, L. Chen, Y. Yue, C. Ye, F. Deng, Acid sites in mesoporous Al-SBA-15 material as revealed by solid-state NMR spectroscopy, Microporous and Mesoporous Materials. 92 (2006) 22–30. https://doi.org/10.1016/j.micromeso.2005.12.013.

[53] B. Girisuta, L.P.B.M. Janssen, H.J. Heeres, Green chemicals: A kinetic study on the conversion of glucose to levulinic acid, Chemical Engineering Research and Design. 84 (2006) 339–349. https://doi.org/10.1205/cherd05038.

[54] A.A. Marianou, C.M. Michailof, A. Pineda, E.F. Iliopoulou, K.S. Triantafyllidis, Applied Catalysis A , General E ff ect of Lewis and Brønsted acidity on glucose conversion to 5-HMF and lactic acid in aqueous and organic media, Applied Catalysis A, General. 555

(2018) 75–87. https://doi.org/10.1016/j.apcata.2018.01.029.

[55] I. Jiménez-morales, M. Moreno-recio, J. Santamaría-González, P. Maireles-torres, A. Jiménez-lópez, Applied Catalysis B : Environmental Production of 5-hydroxymethylfurfural from glucose using aluminium doped MCM-41 silica as acid catalyst, "Applied Catalysis B, Environmental." 164 (2015) 70–76. https://doi.org/10.1016/j.apcatb.2014.09.002.

[56] K. Kumar, F. Parveen, T. Patra, S. Upadhyayula, Hydrothermal conversion of glucose to levulinic acid using multifunctional ionic liquids : effects of metal ion co-catalysts on the product yield, (2018) 228–236. https://doi.org/10.1039/c7nj03146g.

[57] X. Li, X. Liu, Comprehensive Understanding of the Role of Brønsted and Lewis Acid Sites in Glucose Conversion into, (2016). https://doi.org/10.1002/cctc.201601203.

[58] L. Hermida, A. Zuhairi, A. Rahman, Synthesis of monoglyceride through glycerol esterification with lauric acid over propyl sulfonic acid post-synthesis functionalized SBA-15 mesoporous catalyst, Chemical Engineering Journal. 174 (2011) 668–676. https://doi.org/10.1016/j.cej.2011.09.072.

[59] C. Pirez, A.F. Lee, J.C. Manayil, C.M.A. Parlett, K. Wilson, Hydrothermal saline promoted grafting : a route to sulfonic acid SBA-15 silica with ultra-high acid site loading for biodiesel synthesis †, (2014) 4506–4509. https://doi.org/10.1039/c4gc01139b.

[60] M. Sasidharan, A. Bhaumik, Journal of Molecular Catalysis A : Chemical Selective conversion of nitroalcohols to nitroolefins over sulfonic acid functionalized mesoporous SBA-15 material, "Journal of Molecular Catalysis. A, Chemical." 367 (2013) 1–6. https://doi.org/10.1016/j.molcata.2012.11.006.

[61] Hydrothermolysis of carbohydrates to levulinic acid using metal supported on porous aluminosilicate Sirinart Suacharoen a and Duangamol Nuntasri Tungasmita b ∗, (2012). https://doi.org/10.1002/jctb.4000.